Available online at www.sciencedirect.com
SCIENCE DIRECT®
PERGAMON
Radiation Measurements 36 (2003) 343–349
Radiation Measurements
www.elsevier.com/locate/radmeas

Remnant magmatic activity in the Coastal Range of East Taiwan after arc–continent collision: fission-track data and $^3He/^4He$ ratio evidence

T.F. Yang*, C-H. Chen, R.L. Tien, S.R. Song, T.K. Liu

Department of Geosciences, National Taiwan University No.1, Sec.4, Roosevelt Road, Taipei 106, Taiwan

Received 21 October 2002; received in revised form 7 January 2003; accepted 29 April 2003

Abstract

The magma activity of the North Luzon Arc is considered to have ceased, due to collision with the Asian continental margin, since late Miocene. New fission track dates of zircons taken from dike swarms in the central Coastal Range of East Taiwan show very young ages of ~0.5 Ma. Furthermore, the high $^3He/^4He$ ratios (~2.5 R_A; R_A is the air ratio) of hot spring gases near the same area indicate that more than 30% of a mantle-derived source component is necessary to account for the helium composition. These results suggest the existence of later remnant magmatic activity (more than 4 Ma) in the central Coastal Range. Therefore, arc magmatism may survive longer than the previously expected after collision.

Keywords: Magma activity; Arc–continent collision; Fission track date; $^3He/^4He$ ratio

1. Introduction

The northern part of the Taiwan–Luzon Arc, which formed in response to the subduction of the South China Sea plate underneath the Philippine Sea plate, is currently colliding with the Eurasian continental plate (Fig. 1). This collision, beginning approximately at 6 Ma, has propagated progressively southward; thus the northern part of the arc has already been accreted onto the continental margin resulting in formation of the Coastal Range in eastern Taiwan (Teng, 1990; Huang et al., 1997). The geochemical characters of the arc lavas also show significant spatial and temporal variation due to the collision (e.g., Lo, 1989; Yang et al., 1996; Yang, 1997). Volcanic activity has ceased gradually from the northern part toward the southern part of the Coastal Range (Lo et al., 1994). Yang et al. (1995) compiled the available radiometric ages (K–Ar, FT and Ar–Ar) of volcanic rocks in the Coastal Range of East Taiwan and concluded that they range from 16 to 2.2 Ma. These eruption ages become systematically younger trending from the north towards the collision zone in the southern part of the Range (Fig. 1). This evidence supports the model that the arc magmatism may gradually become extinct within 1–2 Ma after arc–continent collision (Dorsey, 1992; Song and Lo, 2002). In this study, we demonstrate that the arc magmatism after collision may survive longer than the previously expected, at least in this area, based on the results of new fission track (FT) dates and helium isotopic data of gas samples from hot springs and mud volcanoes.

2. Analysis and results

2.1. Fission-track dating experimental method

Zircon grains separated from the samples were mounted parallel to their *c*-axis in perfluoralkoxyethylene (PFA) teflon sheets, carefully ground with fine calcite powders, and then etched with a mixture of NaOH, KOH, and $LiOH \cdot H_2O$ (6:14:1 mol%; Zaun and Wagner, 1985) at 200±5°C for 30 ± 5 h. Track counting was conducted at a

* Corresponding author. Tel.: +886-2-3366-5874; fax: +886-2-2363-6095.
E-mail address: tyyang@ccms.ntu.edu.tw (T.F. Yang).

1350-4487/03/$ - see front matter
doi:10.1016/S1350-4487(03)00149-5

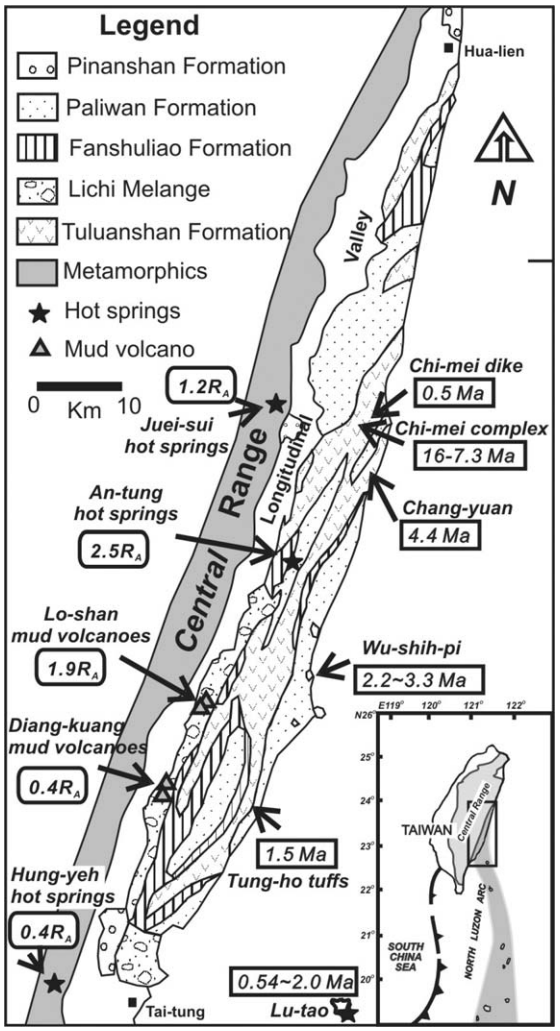

Fig. 1. Zircon fission track ages (this study and Yang et al., 1995) and the $^3He/^4He$ ratios of gases from hot springs and mud volcanoes in the Coastal Range, East Taiwan. (A) Simplified tectonic setting around Taiwan; (B) Geological map of the Coastal Range. Note that Jin-lun hot springs, which is located at 40 km south of Hung-yeh hot springs, is not shown in the figure.

magnification of 2500 under oil immersion. The grain-by-grain mica external detector technique was adopted to determine individual grain ages.

Two pieces of standard glass NBS SRM-610 or SRM-612, which have been calibrated against the fission-track age standard—Fish Canyon Tuff (Naeser et al., 1981) were wrapped tightly and irradiated together with the samples. The zeta (ζ) value (Hurford and Green, 1983) for the standard glass SRM-612 and SRM-610 were evaluated to be 340 ± 12 (1σ) and 27.9 ± 1.5 (1σ) (ya cm^2), respectively. The former is comparable to the value of 339 ± 10 (2σ) by Hurford and Green (1983) and 342.1 ± 6.2 (2σ) by Tagami (1987).

Fission-track grain ages (T_{unk}) were calculated using the equation:

$$T_{unk} = \frac{1}{\lambda_d} \ln\left[1 + \left(\frac{\rho_s}{\rho_i}\right) \lambda_d \rho_d \xi\right]$$

where λ_d is the total decay constant of uranium (1.551×10^{-10} ya^{-1}; Jaffey et al., 1971) and ρ_d is the detector track density from the standard glass dosimeter (tracks/cm^2). Uncertainties in ages were calculated from the Poisson uncertainties in N_s, N_i, N_d and ζ value in the manner described by Green (1981). The final fractional uncertainty in grain age T is

$$\frac{\sigma(T)}{T} = \left\{\frac{1}{N_s} + \frac{1}{N_i} + \frac{1}{N_d} + \left[\frac{\sigma(\zeta)}{\zeta}\right]^2\right\}^{1/2},$$

where N_s and N_i denote the number of spontaneous and induced tracks counted, in each crystal and N_d is the number of induced tracks registered in a mica detector irradiated against the standard glass dosimeter. The detailed handling and analytic procedures and age calculations have been described by Liu et al. (2000, 2001).

2.2. Fission-track dating result

Two samples were collected for FT analysis from the Chi-mei dike swarms in the central Coastal Range (Fig. 1). Because of the aphyric texture, only few grains of zircon were able to be separated from these dike rocks even though the sample weights were up to 15 kg for each specimen. Three and eight zircon FT grain ages were determined for each sample respectively (Table 1). A pooled age of 0.5 ± 0.1 Ma was calculated for sample CM-d2. Using the program of Brandon (2002), we present the probability density plot (Hurford et al., 1984; Brandon, 1996) and radial plot (Galbraith, 1990) of the sample to display the spread of individual grain ages (Fig. 2), in which a cluster of grain ages of ~0.5 Ma is shown. The other grain ages fall within the range of 1σ standard error and the sample passes the χ^2 test with 92.5% probability (Table 1). Moreover, a peak age of 0.6 Ma obtained in the probability density plot (Fig. 2A) is consistent with the pooled age of 0.5 ± 0.1 Ma. This confirms that the pooled age represents the intrusion age of the dikes.

Although there are not enough single grain ages to yield a meaningful pooled age for sample CM-d1 (Table 1), two grain ages of 0.5 and 0.6 Ma are consistent with the pooled age for sample CM-d2. This result supports that the intrusion age of around 0.5 Ma for the Chi-mei dike. Nevertheless, an old grain age of 39 ± 14 Ma was derived in this sample. Some old FT zircon grain ages were also found in some lavas of North Luzon arc. Combined with the evidences of petrographic texture, xenoliths occurrence, and disequilibrium of mineral and radiogenic isotopic compositions, Yang et al. (1995) concluded those FT ages with bimodal distributions in probability density plot may be partial annealed inherited ages due to crustal contamination. This abnormally old age of this

Table 1
Fission-track dating results of Chi-mei dike in the Coastal Range, E. Taiwan

Sample no.	Grain no.	Spontaneous tracks		Induced tracks		$P(\chi^2)$	Glass monitor		Age $\pm 1\sigma$ (Ma)
		ρ_s	(N_s)	ρ_i	(N_i)	(%)	ρ_d	(N_d)	
CM-d1	1	4.40×10^4	(4)	3.05×10^6	(277)		1.40×10^6	(4512)	0.6 ± 0.3
	2	9.58×10^4	(2)	8.14×10^6	(170)		1.40×10^6	(4512)	0.5 ± 0.4
	3	5.94×10^5	(16)	5.94×10^5	(16)		1.40×10^6	(4512)	39 ± 14[a]
	Pooled	1.59×10^5	(22)	3.34×10^6	(463)	< 1	1.40×10^6	(4512)	1.9 ± 0.4
CM-d2	1	5.35×10^3	(2)	1.80×10^6	(671)		4.26×10^6	(2576)	0.4 ± 0.3
	2	6.60×10^3	(4)	1.50×10^6	(907)		4.26×10^6	(2576)	0.5 ± 0.3
	3	4.95×10^3	(3)	1.37×10^6	(831)		4.26×10^6	(2576)	0.5 ± 0.3
	4	9.43×10^3	(2)	2.59×10^6	(550)		4.26×10^6	(2576)	0.5 ± 0.4
	5	5.50×10^3	(2)	1.40×10^6	(508)		4.26×10^6	(2576)	0.5 ± 0.4
	6	1.55×10^4	(5)	3.03×10^6	(978)		4.26×10^6	(2576)	0.6 ± 0.3
	7	6.00×10^3	(2)	9.21×10^5	(307)		4.26×10^6	(2576)	0.8 ± 0.6
	8	2.64×10^4	(4)	3.14×10^6	(475)		4.26×10^6	(2576)	1.0 ± 0.5
	Pooled	8.08×10^3	(24)	1.76×10^6	(5227)	92.5	4.26×10^6	(2576)	0.5 ± 0.1

1. Track densities (ρ) are as measured in (tracks/cm^2); numbers of counted tracks (N) are shown in parentheses. 2. $P(\chi^2)$ is probability of obtaining χ^2 value for v degrees of freedom, where $v =$ (number of crystals $-$ 1). Note that possible upward bias in χ^2 probability due to low counts.

[a]The abnormally old age may be derived from either a contaminated zircon grain or an artifact of experiment.

dike sample may be considered as either a contaminated zircon grain from the host andesite during the dike injection, or an artifact during the experimental processes.

2.3. Helium isotopic compositions

The helium isotopic ratios of terrestrial materials can be identified as deriving from four components. (1) Air: its ^{3}He/^{4}He ratio is very homogeneous (1.39×10^{-6}) and is commonly used as global standard (1 R_A); (2) Crust: the helium isotopic ratios are much lower than air (0.1–0.01 R_A) because abundant ^{4}He gases are produced by the radiogenic elements in the crust; (3) Upper mantle: as represented by the mid-ocean ridge basalts (MORB), which show narrow range of helium isotopic ratios (8 ± 1 R_A); (4) Lower mantle: hot spot basalts are believed to have trapped the primordial ^{3}He, and usually exhibit much higher ^{3}He/^{4}He ratios (> 30 R_A). Hence, the helium isotopic ratio is widely used as a useful tool to trace of relevant samples source domain (e.g., Poreda and Craig, 1989).

Utilizing pre-evacuated low permeability glass bottles with two evacuated stopcocks at both ends, representative bubbling gas samples of hot springs and mud volcanoes from eastern Taiwan (Fig. 1) have been collected for the measurement of their gas compositions. ^{3}He/^{4}He and ^{4}He/^{20}Ne ratios have been measured with the Micromass 5400 noble-gas mass spectrometer with dual collectors in the Department of Geosciences, National Taiwan University. Air was routinely run as a standard for calibration. In general, the total errors on the ratios are less than 2% and 5% for ^{3}He/^{4}He and ^{4}He/^{20}Ne, respectively. Details of the measurements have been given by Yang (2000).

The measured helium isotope ratios range from 5.49×10^{-7} to 3.42×10^{-6} (Table 2). ^{3}He/^{4}He ratios for the possible air contamination have been corrected by assuming that all the neon in the samples is derived from air (Poreda and Craig, 1989), and only the corrected ^{3}He/^{4}He ratios are used for discussion in this paper. Our results indicate that samples in the northern part of the studied area, including Juei-sui hot spring (1.19 R_A), An-tung hot springs (2.37–2.54 R_A) and Lo-shan mud volcanoes (1.71–1.89 R_A), exhibit high helium isotopic ratios (Table 2). This implies that a mantle-derived component made an important contribution to their gas sources. On the other hand, samples from further south show much lower ratios. For instance, the helium isotopic compositions of Jin-lun, Hung-yeh hot springs and Diang-kung mud volcanoes are 0.29, 0.49, and 0.39–0.55 R_A, respectively, indicating that a crust component constrains their sources of origin.

3. Discussion

3.1. Mantle source outgassing

Hot springs are common in Taiwan because of the relatively high geothermal gradient in orogenic terranes. Except

Table 2
Helium isotopes data of fluid samples in the Coastal Range, East Taiwan

Sample No.	sample type[a]	$^4He/^{20}Ne$	$^3He/^4He$	R_A[b]	$[R_A]$[c]	±	1σ	[He]ppm
Juei-sui hot springs								
90728-RS-2-1	W	2.5	1.65×10^{-6}	1.19	1.22	±	0.04	1.72
An-tung hot springs								
90409-AT-1	BG	6.5	3.42×10^{-6}	2.46	2.54	±	0.06	—
90728-AT-2-1	BG	9.1	3.23×10^{-6}	2.32	2.37	±	0.06	48.9
00215-AT-2-1	BG	7.7	3.27×10^{-6}	2.35	2.41	±	0.06	48.8
00215-AT-2-1	BG	8.5	3.35×10^{-6}	2.41	2.47	±	0.08	51.9
00915-AT-2-1	BG	10.8	3.33×10^{-6}	2.40	2.44	±	0.07	54.9
20224-AT-2-1	BG	5.4	3.30×10^{-6}	2.38	2.46	±	0.06	37.5
Jin-lun hot springs								
20225-KL-3-1	BG	3.7	3.99×10^{-6}	0.29	0.22	±	0.01	4.26
Hung-yeh hot springs								
90410-HY-1	BG	2.7	6.76×10^{-6}	0.49	0.42	±	0.02	—
Lo-shan mud volcanoes								
90409-LS-1A	BG	22.6	2.59×10^{-6}	1.86	1.88	±	0.05	—
90409-LS-2A	BG	21.2	2.38×10^{-6}	1.71	1.72	±	0.04	—
90409-LS-1C	BG	10.2	2.59×10^{-6}	1.86	1.89	±	0.05	—
90728-LS-2C-1	BG	22.3	2.42×10^{-6}	1.74	1.75	±	0.04	22.0
90728-LS-2A-1	BG	20.3	2.45×10^{-6}	1.76	1.78	±	0.04	15.6
00215-LSa-2-1	BG	56.0	2.54×10^{-6}	1.83	1.83	±	0.06	18.8
00215-LSc-2-2	BG	18.7	2.61×10^{-6}	1.88	1.89	±	0.05	20.3
20224-LS2-2-1	BG	19.5	2.57×10^{-6}	1.85	1.87	±	0.05	24.2
Diang-kuang mud volcanoes								
90409-DK-1	BG	1.1	7.64×10^{-7}	0.55	0.38	±	0.01	—
90409-DK-3	BG	2.2	6.50×10^{-7}	0.47	0.38	±	0.01	—
90728-DK-2-1	BG	12.9	5.49×10^{-7}	0.39	0.38	±	0.01	9.85
00216-DK-2-2	BG	19.5	5.72×10^{-7}	0.41	0.40	±	0.02	9.39
20224-DK-2-1	BG	1.4	7.40×10^{-7}	0.53	0.39	±	0.01	5.65

[a] W, water; BG, bubbling gas.
[b] R_A is the $^3He/^4He$ ratio normalized to the air ratio (1.39×10^{-6}).
[c] $[R_A]_c$ is the air corrected ratio, assuming all the Ne derived from the air (Poreda and Craig, 1989).

for the hydrothermal hot springs in northern Taiwan and offshore islets in SE Taiwan, which are believed to be related to hydrothermal activity, most of the hot springs are distributed in the Central Range and along the deformation front of western Taiwan (Chen, 1989). Yang (2002) recognized that most fluid gases from the Central Range are mixtures of a crustal source with air-saturated groundwater, with few exceptions that may be affected by a mantle-derived component due to the nearby hydrothermal activity in NE Taiwan. Gases collected from the Central Range, with 0.42 R_A for Hung-yeh hot springs and 0.29 R_A for Jin-lun hot springs (Table 2), confirm this conclusion.

An-tung, interestingly, is the only place in the Coastal Range where hot springs can be found (Fig. 1). Helium isotopic data suggests that 30% mantle component mixed with crust component is necessary to account for the helium compositions (Fig. 3). The nearby Juei-sui hot springs in the Central Range also show elevated $^3He/^4He$ ratios which might also be influenced by the same mantle outgassing source as in the central Coastal Range.

In addition to the hot spring, mud volcano gases can also provide useful information to constrain their tectonic environments. Mud volcanoes are widely distributed in southern Taiwan as part of the obduction accretionary prism in the

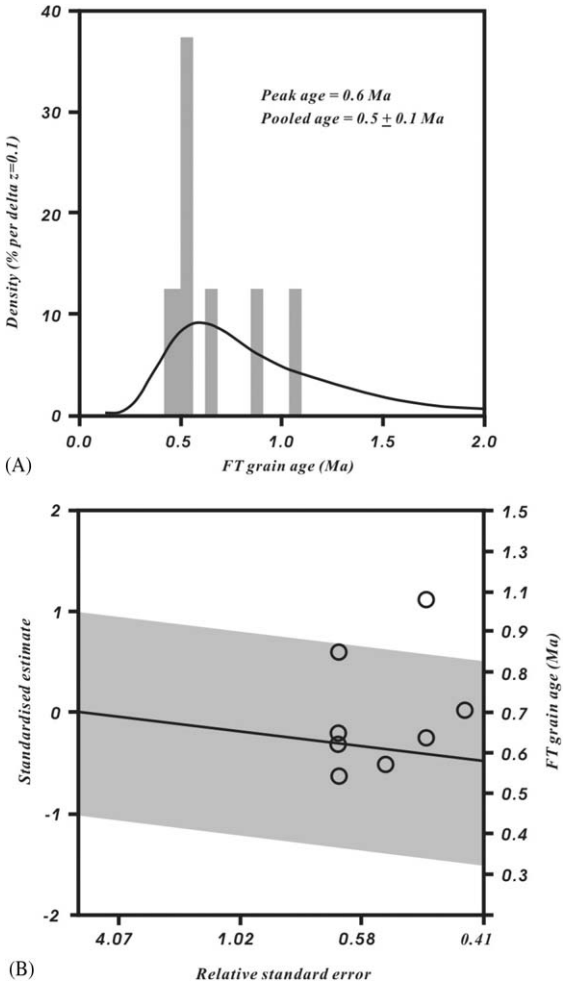

Fig. 2. (A) Probability density plot; and (B) radial plot for the zircon FT single-grain ages for sample CM-d2, the shaded area marks the $\pm 1\sigma$ of the best-fit peak age.

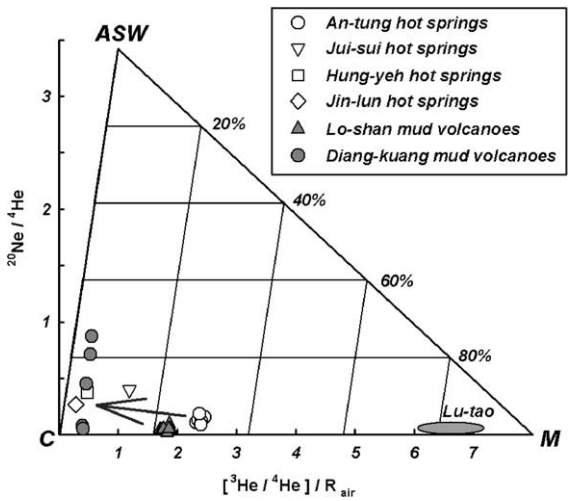

Fig. 3. Three-component plot of helium isotopes of the fluid samples from the Coastal Range, East Taiwan. The arrow indicates the trend of higher $^3He/^4He$ ratios from central Coastal Range towards lower ratios of southern Coastal Range. Lutao hot spring gases, which exhibit significant mantle-derived gas component (Yang, 2002), are also shown for comparison. ASW: air saturated water; C: crust; M: mantle component.

arc–continent collision terrane (Huang et al., 1997; Chang et al., 2000). Yeh et al. (2002) divided the mud volcanoes into five groups based on different tectonic terranes. Furthermore, they suggested that the fluids originated from different sources at different depths. Helium isotopic ratios of the mud volcano gases from southwestern Taiwan range from 0.08 to 0.25 R_A, indicating that the gases originated mostly from the crustal component. This is consistent with the concept that mud volcanoes are part of the accretionary prism dominated by crustal sediment sources. However, these ratios are higher than the typical crustal composition ($\sim$0.02 R_A), so that an upper mantle component ($\sim$8.0 R_A) is necessary to elevate these ratios (Yang, 2002).

In contrast to the relatively low helium isotopic ratios of mud volcanoes gases from SW Taiwan, those from the Coastal Range exhibit much higher helium isotopic ratios in this study. This indicates that more mantle derived component has been involved in their gas compositions, and further implies that a remnant magma source may exist and contribute to the current outgassing system in the Coastal Range. Interestingly, Lo-shan mud volcanoes exhibit higher $^3He/^4He$ ratios than those of Diang-kung mud volcanoes (Fig. 1). With reference of the An-tung hot springs located at north, the helium isotopic ratios of gases display a southward decreasing trend in the Coastal Range (Figs. 1 and 3). This suggests that the mantle outgassing source resides beneath the mud volcanoes in the north, if the remnant magma does exist in this area to significantly influence their gas compositions.

3.2. Arc magmatism in the Coastal Range after arc–continent collision

The Chi-mei Igneous Complex, located in central Coastal Range, is composed mainly of intrusive diabase, dikes, lava flows and pyroclastic rocks. FT zircon ages of 16 ± 1 Ma give the minimum formation age of the Chi-mei Igneous complex (Yang et al., 1988), although the sample has been hydrothermally altered. This age is in agreement with the oldest whole rock Ar–Ar plateau age in the northern part of this Range (16.0 ± 0.2 Ma; Lo et al., 1994). The Chi-mei Igneous Complex is overlain by the Tuluanshan Formation, which includes a series of volcanic and volcaniclastic rocks intercalated with thin layers of marine sediments. The age of the Tuluanshan Formation in the central Coastal Range varies from 16.6 to 5 Ma as dated by K–Ar and fossil ages (Song and Lo, 2002). The youngest age was constrained

from the foraminifera in the top of the tuff layers of the Tuluanshan Formation, which is believed to be the product of last stage eruption in central Coastal Range. This implies that the arc magmatism may have ceased within one Ma after arc–continent collision.

The younger FT dates of Wu-shih-pi lavas (2.2–3.3 Ma) can be used to constrain the time of the arc–continent collision which terminated the magmatism in the southern Coastal Range (Yang et al., 1995). The young dates (1.5 ± 0.1 Ma) obtained for the biotite-tuff from Tung-ho (Fig. 1) may not represent a later magmatic event in the Coastal Range. Yang et al. (1995) suggested that these tuffs were the eruption products from the nearest off-shore island, Lu-tao, where eruptions of biotite–hornblende andesites occurred from 1.8 to 0.54 Ma. Thus, they concluded that the magmatic activity of the Coastal Range commenced earlier than 16 Ma, and ceased about 5 Ma in central part and 2.2 Ma in southern part of the Coastal Range, respectively.

This conclusion is consistent with the observations in other places of the world. Arc magmatism in an arc–trench system usually will be stopped in 1–2 Ma after the collision of buoyant seamounts, ridges or plateaus (Nur and Ben-Avraham, 1989). This will produce a significant volcanic gap due to the discontinuity of the subducting plate (e.g., Nur and Ben-Avraham, 1989; Yang et al., 1996). In some collision areas, the arc magmatism may be continuing after collision and last up to 20 Ma, if the continental plate itself was subducted and involved in magma generation, e.g., Gangdese in Himalayan area (Copeland et al., 1995). Since there is no evidence of continuing subducting plate underneath the Coastal Range, hence, no magmatism would be expected to survive in this stage (Huang et al., 1997). However, our study provides new data to reveal that this may not be a general case.

The unexpectedly young FT ages of 0.5 Ma obtained from the Chi-mei dike swarms indicate that magmatism occurred just very recently in the central Coastal Range. It implies that arc magmatism may still survive more than four million years, which is longer than previously expected, after the onset of arc–continent ($\sim$5 Ma) in this area. Systematic spatial helium isotopic variations of gases also support the conclusion that remnant magma source may exist and still outgas in the central Coastal Range.

4. Conclusion

The young zircon FT age of 0.5 ± 0.1 Ma for the Chi-mei dike swarms obtained in this study strongly suggests that there was some remnant magmatism, at least in the central Coastal Range, longer than 4 Ma after the arc–continent collision occurred in this area. This is supported by the helium isotopic results of the gases emanated in the same area, indicating that more than 30% mantle-derived source component is necessary to account for the helium compositions of hot springs and mud volcanoes. In conclusion, we propose that the remnant magma source was located in the central Coastal Range. This could lead to a high geothermal gradient and provide the necessary mantle source for the gas compositions.

Acknowledgements

The authors wish to thank Ms. P.S., Hsieh, Mrs. N.T. Liu, R.H. Tsai, H.H. Ho, G.H. Yeh, and J.H. Jiang for helping in sample collection and analysis, and Dr. C.-y. Lee arranging for the irradiation of zircon samples. This paper was much improved by two anonymous reviewers who made critical reviews and comments. This study was partly financially supported by the National Science Council, Taiwan, ROC (NSC90-2116-M-002-031/TFY).

References

Brandon, M.T., 1996. Probability density plot for fission-track grain-age samples. Radiat. Meas. 26, 663–676.

Brandon, M.T., 2002. Decomposition of mixed grain age distributions using BINOMFIT. On Track 24, 13–18.

Chang, C.P., Angelier, J., Huang, C.Y., 2000. Origin and evolution of a melange: the active plate boundary and suture zone of the Longitudinal valley. Taiwan. Tectonophysics 325, 43–62.

Chen, C.H., 1989. Hot springs and geothermal energy in Taiwan. Ti-Chih 9, 327–340 (in Chinese with English abstract).

Copeland, P., Harrison, T.M., Kidd, W.S.F., Xu, R., Zhang, Y., 1995. Thermal evolution of the Gangdese batholith, southern Tibet: a history of episodic unroofing. Tectonics 14, 223–236.

Dorsey, R.J., 1992. Collapse of the Luzon volcanic arc during onset of arc–continent collision: evidence from a Miocene–Pliocene unconformity, eastern Taiwan. Tectonics 11, 177–191.

Galbraith, R.F., 1990. The radial plot: graphical assessment of spread in ages. Nucl. Tracks Radiat. Meas. 17, 207–214.

Green, P.F., 1981. A new look at statistics in fission-track dating. Nucl. Tracks 5, 77–86.

Huang, C.Y., Wu, W.Y., Chang, C.P., Tsao, S., Yuan, P.B., Lin, C.W., Xia, K.Y., 1997. Tectonic evolution of accretionary prism in the arc–continent collision terrane of Taiwan. Tectonophysics 281, 31–51.

Hurford, A.J., Green, P.F., 1983. The zeta calibration of fission track dating. Isot. Geosci. 1, 285–317.

Hurford, A.J., Fitch, F.J., Clarke, A., 1984. Resolution of the age structure of the detrital zircon populations of two Lower Cretaceous sandstones from the Weald of England by fission track dating. Geol. Mag. 121, 269–277.

Jaffey, A.H., Flynn, K.F., Glendenin, L.E., Bentley, W.C., Essling, A.M., 1971. Precision measurements of half-lives and specific activities of ^{235}U and ^{238}U. Phys. Rev. C 4, 1889–1906.

Liu, T.K., Chen, Y.G., Chen, W.S., Jiang, S.H., 2000. Rates of cooling and denudation of the Early Penglai Orogeny, Taiwan, as assessed by fission-track constraints. Tectonophysics 320, 69–82.

Liu, T.K., Hsieh, S., Chen, Y.G., Chen, W.S., 2001. Thermo-kinematic evolution of the Taiwan oblique-collision mountain belt as revealed by zircon fission track dating. Earth Planet. Sci. Lett. 186, 45–56.

Lo, C.H., Onstott, T.C., Chen, C.H., Lee, T., 1994. An assessment of $^{40}Ar/^{39}Ar$ dating for the whole-rock volcanic samples from the Luzon Arc near Taiwan. Chem. Geol. 114, 157–178.

Lo, H.J., 1989. Evolution of the volcanic arcs of the Coastal Range, eastern Taiwan. Acta Geol. Taiwan 27, 1–18.

Naeser, C.W., Zimmermann, R.A., Cebula, G.T., 1981. Fission track dating of apatite and zircon: an interlaboratory comparison. Nucl. Tracks 5, 65–72.

Nur, A., Ben-Avraham, Z., 1989. Oceanic plateaus and the Pacific ocean margins. In: Ben-Avraham, Z. (Ed.), The Evolution of the Pacific Ocean Margins. Oxford University Press, New York, pp. 3–19.

Poreda, R., Craig, H., 1989. Helium isotope ratios in Circum-Pacific volcanic arcs. Nature 338, 473–478.

Song, S.R., Lo, H.J., 2002. Lithofacies of volcanic rocks in the central Coastal Range, eastern Taiwan: implications for island arc evolution. J. Asian Earth Sci. 21, 23–38.

Tagami, T., 1987. Determination of zeta calibration constant for fission track dating. Nucl. Tracks Radiat. Meas. 13, 127–130.

Teng, L.S., 1990. Geotectonic evolution of late Cenozoic arc–continent collision in Taiwan. Tectonophysics 183, 57–76.

Yang, T.F., 1997. Origin and geodynamic implication of the Dupal isotopic anomaly in volcanic rocks from the Philippine arcs: Comment. Geology 25, 284.

Yang, T.F., 2000. The helium isotopic ratios of fumaroles from Tatun Volcano Group of Yangmingshan National Park, N. Taiwan. J. Nat. Park 10, 73–94 (in Chinese with English abstract).

Yang, T.F., 2002. $^{3}He/^{4}He$ ratios of fluid samples in Taiwan. Geochim. Cosmochim. Acta 66, A859.

Yang, T.Y., Liu, T.K., Chen, C.H., 1988. Thermal event records of the Chi-mei Igneous Complex: constraint on the ages of magma activities and the structural implication based on fission track dating. Acta Geol. Taiwan 26, 237–246.

Yang, T.F., Tien, J.L., Chen, C-H., Lee, T., Punongbayan, R.S., 1995. Fission-track dating of volcanics in the northern part of the Taiwan–Luzon Arc: eruption ages and evidence for crustal contamination. J. SE Asian Earth Sci. 11, 81–93.

Yang, T.F., Lee, T., Chen, C-H., Cheng, S.N., Knittel, U., Punongbayan, R.S., Rasdas, A.R., 1996. A double island arc between Taiwan and Luzon: consequence of ridge subduction. Tectonophysics 258, 85–101.

Yeh, G.H., You, C.F., Chen, J.C., Yang, T.F., Chen, Y.G., Song, S.R., 2002. Fluid geochemistry of mud volcanoes at the accretionary prism in southern Taiwan. Geochim. Cosmochim. Acta 66, A862.

Zaun, P.E., Wagner, G.A., 1985. Fission-track stability in zircons under geological conditions. Nucl. Tracks 10, 303–307.